Solid bones in large animals: a microanatomical investigation

Alexandra Houssaye[1,*]
* Corresponding author
Email: houssaye@mnhn.fr

Katja Waskow[2]
Email: waskow@uni-bonn.de

Shoji Hayashi[3]
Email: hayashi@mus-nh.city.osaka.jp

Raphaël Cornette[4]
Email: cornette@mnhn.fr

Andrew H. Lee[5]
Email: alee712@gmail.com

John R. Hutchinson[6]
Email: JHutchinson@rvc.ac.uk

[1]*UMR 7179 CNRS/Muséum National d'Histoire Naturelle, Département Ecologie et Gestion de la Biodiversité, 57 rue Cuvier CP-55, 75000 Paris, France*
[2]*Steinmann Institut für Geologie, Mineralogie und Paläontologie, Universität Bonn, Nussallee 8, 53115 Bonn, Germany*
[3]*Osaka Museum of Natural History, Higashi-sumiyoshi-ku, Osaka, 546-0034, Japan*
[4]*UMR CNRS/MNHN/UPMC/EPHE 7205, Institut de Systématique, Evolution, Biodiversité (ISYEB), Muséum National d'Histoire Naturelle, 45 rue Buffon, 75005 Paris, France*
[5]*Department of Anatomy, Midwestern University, 19555 N 59th Avenue, Glendale, AZ 85308, USA*
[6]*Department of Comparative Biomedical Sciences, Structure and Motion Laboratory, The Royal Veterinary College, Hatfield, United Kingdom*

Abstract

Background

Graviportal taxa show an allometric increase of the cross-sectional areas of supportive bones and are assumed to display microanatomical changes associated with an increase in bone mass, presumably to offer greater resistance to loads produced by their gigantic size. This evokes osteosclerosis, i.e., an increase in bone compactness, that is also observed in some aquatic amniotes. This study investigates the changes in bones' inner structure associated with graviportality and how comparable they are with aquatically acquired osteosclerosis in order to better understand the adaptation of bone to the different functional requirements associated with graviportality in giant tetrapods, and with buoyancy and body trim control in secondarily aquatic tetrapods.

Results

This microanatomical and cross-sectional investigation of long bones and ribs of graviportal and other related tetrapod taxa shows changes of inner structure that are not solely attributable to allometry. Bones of graviportal taxa display a thicker cortex and a proportionally smaller medullary cavity, with a wider transition zone between these domains. This inner cancellous structure may enable better impact energy absorption and marrow support. Moreover, the cross-sectional geometric parameters indicate increased resistance to stresses engendered by bending and torsion as well as compression.

Conclusions

Although not all graviportal taxa converge on the same inner organization of their bones, a clear general pattern is evident across graviportal tetrapods. The increase in bone mass, although it might be mistaken with aquatically related osteosclerosis, is nevertheless more restricted than the osseous specialization observed in some shallow water swimmers or bottom-walkers among almost exclusively aquatic amniotes. Adaptation to a graviportal posture should thus be taken into consideration when analysing possibly amphibious taxa with a terrestrial-like morphology. This consideration is particularly important for paleoecological inferences about large extinct tetrapods that might have been amphibious and, more generally, for the study of early stages of adaptation to an aquatic life in amniotes.

Keywords

Graviportality, Stylopod, Ribs, Bone mass increase, Osteosclerosis, Gigantism, Amphibious adaptation

Background

Animals with extremely large body masses and with massive pillar-like limbs adapted to support their weight are said to be graviportal [1, 2]. Their typically columnar limbs help to resist bending and torsional loads generated by flexion and rotation of the limbs during locomotion [3–5]. They also display proportionally much longer stylopodial elements (humerus, femur), relatively to the more proximal zeugopodials and autopodials, and, especially, limb bones of much larger diameter. These larger bones result from allometric changes that help them to resist gravity [2, 6, 7], because body mass (and thus gravitational loading) tends to increase by a factor of eight when body length proportionately increases by a factor of two ([8]; p. 43).

The allometric increase of the cross-sectional areas of supportive bones is a well-known characteristic of graviportal vertebrates [9]. However, further adaptations at the microstructural scale may occur -- for example, Doube et al. ([10]) showed how the trabecular mesh of larger species becomes more robust across a wide range of lineages of terrestrial tetrapods. Oxnard [11, 12] posited that there may be a general trend in some graviportal tetrapods to fill in the marrow cavities of the long bones in order to not only resist compressive loads from gravity but also to help absorb more kinetic energy when the feet impact the ground (see Warner et al., 2012), avoiding “crushing fractures”, as well as to provide scaffolding to support the heavy bone marrow itself.

Graviportal long bones and ribs are thus considered more massive than in other terrestrial taxa ([2, 13]) and should show an increase in bone mass at the microanatomical scale. The aforementioned increase in bone mass in graviportal land animals may be analogous to osteosclerosis observed in comparable bones of aquatic amniotes. These secondarily aquatic tetrapods are generally shallow water swimmers relying on a hydrostatic control of buoyancy and body trim (see [14]). Thus, ironically, the increased compactness of bones seems to have convergently evolved multiple times in tetrapods to: (1) maintain

appropriate buoyancy and balance in water, a low-gravity environment, as compared to land; and (2) improve resistance to gravity, enabling the limits of body size in terrestrial tetrapods to be pushed to greater extremes (e.g., Hokkanen, REF). Indeed, Wall [15] already observed that some graviportal taxa seem to show an increase in bone deposition, so that they can be mistaken for aquatic taxa, especially bottom-walkers. In mustelids, the observation of high density in the bones of wolverines seems more associated with their increased body mass than with aquatic habits [16]. Moreover, the high compactness in the ribs of rhinoceroses [17] also illustrates this trend, in combination with varying aquatic habits in extant and extinct rhinocerotoids (Prothero, 1992; [18]REFS).

Here, we investigate microanatomical and cross-sectional specializations in the bones of graviportal and other related tetrapod taxa with both qualitative and quantitative methods, and in a phylogenetic context because microanatomical structures can show phylogenetic signal [19]. We first seek to evaluate the bone microanatomical changes observable in graviportal taxa and to determine how comparable this pattern is to the specialization observed in aquatic amniotes. We then synthesize our comparative results in order to better understand the adaptation of bone to the different functional requirements associated with graviportality in giant tetrapods, and notably focus on how the resulting patterns in graviportal taxa may sometimes be similar to changes associated with buoyancy and body trim control in secondarily aquatic tetrapods.

Institutional abbreviations

AMP: Ashoro Museum of Paleontology, Hokkaido, Japan; BYU: Brigham Young University, Utah, USA; CMC: Cincinnati Museum Center, Ohio, USA; FMNH: Field Museum of Natural History, Chicago, Illinois, USA; HMNS: Hayashibara Museum of Natural Sciences, Okayama, Japan; JRHRVC: uncatalogued research collection of John R. Hutchinson at The Royal Veterinary College, Hatfield, United Kingdom; MDE: Musée des Dinosaures, Espéraza, France; MNHN: Museum national d'Histoire naturelle, Paris, France; MPC: Mongolian Paleontological Center, Ulaanbaatar, Mongolia; NHMUK: Natural History Museum, London, United Kingdom; NMB: Naturhistorisches Museum Basel, Switzerland; NMW: National Museum of Vienna, Austria; NSM: National Science museum, Tokyo, Japan; OMNH: Sam Noble Oklahoma Museum of Natural History, USA; OMNH*: Osaka Museum of Natural History, Osaka, Japan; PIMUZ: Paläontologisches Institut und Museum, Universität Zürich, Switzerland; RTMP: Royal Tyrrell Museum of Palaeontology, Drumheller, Canada; SMA: Sauriermuseum Aathal, Switzerland; STIPB Steinmann-Institut,

Universität Bonn, Germany; UCMP: University of California Museum of Paleontology, USA; UFGK: Ur- und Frühgeschichte Köln, Köln, Germany; UMNH: Utah Museum of Natural History, USA; UMZC: University Museum of Zoology, Cambridge, United Kingdom; YPM: Yale Peabody Museum of Natural History, New Haven, Connecticut, USA; ZFMK: Zoologisches Forschungsmuseum Alexander Koenig, Bonn, Germany; ZMZ, Zoologisches Museum der Universität Zürich, Switzerland.

Results

Qualitative analysis

Humerus

Most taxa exhibit humeri showing the standard tubular structure for a tetrapod long bone; i.e., a layer of compact cortex surrounding a large open medullary cavity (Fig. 1A). The cortex is thicker in the bipedal dinosaurs (the theropods *Tarbosaurus*, *Allosaurus* and the thyreophoran *Scutellosaurus*) and in the nilgai (*Boselaphus*) and the African buffalo (*Syncerus*) than in most tubular bones. The pygmy hippopotamus *Choeropsis* (which is only poorly amphibious; Wall [15]) also displays a tubular bone organization without a particularly thick cortex (Fig. 1B). The tapir shows a wide transition zone between the cortex and the open medullary cavity, and the polar bear shows a thin cortex associated with a wide transition zone (as described in [20]). The giant anteater (*Myrmecophaga*) displays a wide loose spongiosa with no open medullary cavity; and the southern tamandua shows a similar organization but with a rather small open medullary cavity. The peculiarity of the microanatomical features of these Xenarthra taxa was already raised in Straehl et al. ([21]) and Amson et al. [22], matching similar observations of other Xenarthra by Oxnard ([11, 12]).

Among the other taxa sampled, several types of inner organization are observable: 1) absence of an open medullary cavity but a relatively wide medullary area occupied by a spongiosa (higher number of, and thinner osseous trabeculae than in the two xenarthrans above); in *Hippopotamus* (Fig. 1C), the sauropods *Ampelosaurus* (Fig. 1D) *Apatosaurus* and the ceratopsian *Centrosaurus* (Fig. 1E); 2) a similar pattern but associated with a much thicker cortex; in *Ceratotherium* (Fig. 1F), *Rhinoceros unicornis* (Fig. 1G) and *R. sondaicus*, the elephantiform proboscidean *Stegodon*-- and with a reduced open medullary cavity, in one

specimen of *Dicerorhinus*; 3) a thick cortex and a narrow medullary cavity with only a few thick trabeculae; in the extant proboscideans *Elephas* (Fig. 1H) and *Loxodonta*, the rhinocerotids *Dicerorhinus* (one specimen), *Diceros* (Fig. 1I) and *Diceratherium* and the ceratopsian *Protoceratops*. The latter (third) kind of inner bone organization was already observed in the sirenian *Trichechus* [20] (Fig. 1J), whereas the two other relatively slow swimmers sampled, the desmostylian *Paleoparadoxia* (Fig. 1K) and the sirenian *Dugong* (Fig. 1L), display an extremely compact structure with no medullary cavity.

Femur

As observed for the humerus, most taxa display a tubular structure of the femoral midshaft (Fig. 2A). There are substantial variations in the thickness of the cortex, being relatively maximal in *Syncerus* (Fig. 2B) and *Ursus thibetanus*. In the giant anteater, the femur exhibits a pattern similar to its humerus, whereas in the tamandua the femur shows a better defined and larger open medullary cavity than its humerus. Most other taxa have a cortex with a thickness similar to the maximum values observed in the taxa displaying a tubular structure, but with a spongiosa occupying the whole medullary area; for example, in *Ceratotherium*, *Rhinoceros unicornis* (Fig. 2C), *Rhinoceros sondaicus* (Fig. 2D) but also in the tapir. Similar to pattern observed in the humerus, other taxa show a thick cortex and a medullary area occupied by a medullary cavity with no or only a few thick trabeculae; in *Elephas* (Fig. 2E), *Loxodonta*, *Mammuthus* (Fig. 2F), *Hippopotamus* (Fig. 2G) and *Ceratotherium* (one specimen). *Diceratherium* shows an inner organization that is almost tubular, except that a rather poorly extended transition zone between the cortex and the medullary cavity is occupied by a spongiosa. *Stegosaurus* (Fig. 2H) shows a thick cortex and a reduced medullary area with a small medullary cavity and a lightly built spongiosa.

Rib

In amniotes, there is a high diversity of rib internal morphologies, notably in the thickness of the cortex and the number of infilling trabeculae, as already highlighted in Hayashi et al. [20]. This reflects a natural diversity but also relies on the difficulty of making homologous comparisons with ribs, as bone microanatomical features are known to vary both along the rib and between ribs along the ribcage (e.g., [23, 24]).

Typically in our sample, the ribs of quadrupedal taxa show a clear medullary area with no or a few thick trabeculae (Fig. 3A-B). Weakly active swimmers are characterized by a clear increase in bone compactness, which is limited in most desmostylians (Fig. 3C) but

extremely high in all sirenians (*Trichechus*, *Dugong* and *Halitherium*; AH unpublished observations) with an almost complete bone filling. Most dinosaurian taxa sampled, especially graviportal thyreophorans (stegosaurs [Fig. 3D] and ankylosaurs) and sauropods (Fig. 3E-F), but also bipedal taxa (Fig. 3G), display ribs with a thick cortex and no open medullary cavity, but rather a dense spongiosa with reduced intertrabecular spaces in most taxa (Fig. 3D-E). However, some dinosaur taxa present a thick cortex but a rather loose inner spongiosa (e.g., the sauropod *Spinophorosaurus* and the moderately large theropod *Lourhinhanosaurus*; Fig. 3F). The mammoth specimen and *Rhinoceros* (*R. unicornis* and *R. sondaicus*) show an organization grossly similar to that of other large quadrupedal mammals, except that the spongiosa is made of numerous rather thin trabeculae (Fig. 3H-I).

Quantitative analyses

The K statistics calculated are all much lower than 1 for all three bones analysed ($0.34<K<0.68$ for the humerus, $0.37<K<0.55$ for the femur, and $0.39<K<0.67$ for the rib; see Suppl. 1). However, randomization tests are unable to reject the possibility of a significant phylogenetic signal in the data, except for C, S and CSS for the rib. This justifies the need to account for the effects of phylogenetic pseudoreplication [23].

Linear regressions on the independent contrast data show that only J is affected by size (MD) for the three bones, but not strongly. The other parameters show either no or a rather weak impact of size, depending on the bones concerned (see Suppl. 1).

Analyses of variance show that only the parameters C and P for the humerus vary significantly (Table 4) depending on the group number (1-4). Analyses of covariance all show a significant signal when phylogeny is not taken into consideration (except the parameter J for the rib), but lose this significance when phylogeny is incorporated (Table 4). Similarly, the multivariate analyses of variance are significant for the humeri and the femora ($F=2.83$, $p=0.021$ for the humeri; $F=6.00$, $p<0.001$ for the femora; $F=1.99$, $p=0.12$ for the ribs) but become not significant when phylogeny is taken into consideration ($F=5.41$, $p=0.284$ for the humeri; $F=6.20$, $p=0.668$ for the femora; $F=2.77$, $p=0.730$ for the ribs). Bone compactness is greater in aquatic and graviportal (especially in the femur) taxa, which also show a wider transition zone (high S; except in the ribs of the graviportal taxa). Bipedal taxa also display compact ribs with a wide transition zone and a thicker cortex. Aquatic taxa have a more reduced medullary cavity (lower P) associated with a proportionally thicker cortex (low R/t).

This reduced medullary cavity and thicker cortex are also observed, but to a much lesser extent, in graviportal taxa but only in long bones (especially in the femur), not in the ribs. The cross-sectional shape index (CSS) evidences different signals depending on the bone sampled. The polar second moment of area (J) reveals higher values for aquatic (for the humerus; lower values in the ribs), graviportal and bipedal taxa.

Our PCA of bone microanatomy in the humerus shows that the two main axes explain 77.9% of the variance (58.5 and 19.4% respectively). This analysis demonstrates which variables co-varied: P and R/t correlate inversely to C (compactness). The smaller medullary cavity in aquatic and graviportal tetrapods is thus consistently associated with a relatively thicker cortex and a higher compactness values (Fig. 4A). It is particularly interesting to note that graviportal taxa group together (and with aquatic taxa), being essentially discriminated by the first axis, whereas they are randomly distributed based on PC2 and PC3. Our between-groups PCAs generally show for all bones that the first axis mainly discriminates based on bone microanatomical features (C, S, P, R/t), and the second axis essentially based on bone shape parameters (CSS and J; Fig. 4B,5B,6B). The between-groups PCA for the humerus distinguishes the four groups, with aquatic taxa displaying the strongest compactness, thicker cortex, smaller medullary cavity, and more rounded geometry (CSS closer to 1; as opposed to quadrupedal taxa with CSS diverging from 1). Additionally, graviportal taxa, as opposed to bipedal and aquatic ones, display (for obvious reasons of gravitational support) a higher polar second moment of area (J) and larger transition zone between the cortex and medullary cavity (Fig. 4B). The two main axes explain 95.0% of the variance (79.2 and 15.8%, respectively). Our K-NN classifications indicate that 74.5% of specimens were well-classified and thus show a clear and doubtless signal.

Similar to the humerus, our PCA analysis for the femur shows that the two main axes explain 81.0% of the variance in our microanatomical data (64.7 and 16.3% respectively). Similar co-variations are observable between C, P, and R/t. However CSS in this case vary almost antagonistically to P and R/t. Again, graviportal taxa group together, being discriminated based essentially on the first axis (Fig. 5A). The between-groups PCA for the femur shows that graviportal taxa are distinct from the other quadrupedal and the bipedal taxa in showing a much higher compactness, proportionally thicker cortex, and higher polar second moment of area (Fig. 5B). Bipedal taxa differ from quadrupedal ones in showing a higher polar second moment of area (J) and less rounded cross-sections (CSS further from 1). The two main axes explain 100% of the variance, 95.8 and 4.2%, respectively, showing that the variation conclusively distinguishes graviportal taxa from the others. Congruent with our

results for the humerus, we find from the K-NN classifications that we reliably assigned 69.8% of our specimens to groups *a priori*.

The PCA analysis for the ribs shows that the two main axes explain 67.6% of the variance (50.6 and 17.0% respectively). In our rib sample, C still varies antagonistically to R/t and P, and in a direction almost orthogonal to those of the polar second of moment area and cross-sectional shape (Fig. 6A). Graviportal taxa continue to group together. However it is interesting to note that the bipedal taxa are within the distribution area of the graviportal ones and that the two aquatic taxa are much closer to the graviportal forms than to the other terrestrial ones. For ribs, the first axis does not clearly distinguishes graviportal taxa since aquatic and bipedal ones display in fact a much higher compactness, whereas graviportal taxa display microanatomical features closer to those of the other terrestrial forms. The second axis discriminates graviportal taxa from the other ones, notably based on the more rounded shape of the cross-sections (in contrast to the increased eccentricity evident for the humerus and femur; also see [24]) and higher polar second moment of area. These two main axes explain 97.4% of the variance, 68.1and 29.3%, respectively. For ribs, we obtained a relatively poor result for the K-NN classifications: 46.2% of specimens as well-classified.

Comparisons between the classical and between-groups PCAs show that the same parameters drive the distributions of data for both the mean representatives of the groups and for all individuals.

Discussion

We found that only certain key microanatomical and cross-sectional traits distinguish how humeri, femora and ribs of tetrapods change their shape and internal bone structure with increasing graviportal or aquatic adaptations. In particular, the ribs show stronger changes of compactness with aquatic habits than with graviportality. Otherwise, as we proposed in the Introduction, there are remarkable qualitatively and quantitatively similar patterns in how bones change their internal geometry with lifestyles as different as giant, graviportal land animals vs. secondarily aquatic tetrapods, especially increasing bone compactness and reduced medullary cavities along both evolutionary trajectories. As for bipedal taxa, they tend to show a strong change in femoral cross-sectional area and an increased internal robustness in their ribs.

Phylogenetic signal

Our quantitative analyses show that there is a phylogenetic signal in the dataset for most parameters, but that it is somewhat weak. Despite its relative weakness, when phylogeny is taken into consideration, our analyses of (co)variance do not show any significant change between the four groups defined. Although a historical signal is common in bone cross-sectional geometry and microanatomical data, as previously mentioned (e.g. [25]), our findings might also reflect the fact that adaptations to an aquatic lifestyle and to a graviportal morphology occurred only infrequently in amniote evolution, so that the extant taxa showing such adaptations form a few groups on the phylogeny. More thorough sampling of Tetrapoda might show a different phylogenetic signal -- our dataset of <75 total species is far from comprehensive. Our results, however, might still reveal the the occurrence of fundamental trends of anatomical construction that transcend phylogenetic constraints.

Cross-sectional geometry versus microanatomical parameters

Various comparative studies have focused on long bone sections in order to analyse the link between inner bone structure and the structural and functional requirements of extant organisms and to make inferences about the lifestyle of extinct taxa (e.g., [26–29]). Of course, individual bones-- let alone whole skeletons-- of extinct taxa are not always complete. Given the fragmentary nature of fossil material, body size or mass is difficult to estimate precisely. Our aim was to determine how similar the cross-sectional geometry of tetrapod bones is across a continuum encompassing bipedal, quadrupedal, graviportal and aquatic forms with a particular focus on graviportal taxa. In addition to the microanatomical parameters commonly used, we included some cross-sectional geometry parameters. As linear regressions on the independent contrast data showed a strong impact of body size (i.e., maximal diameter) on parameters Per, CSA and Zpol, the latter were considered to display redundant information and were removed from further analyses. However, the parameters J and CSS showed their own patterns of variability and are of appreciable interest in such comparative studies (see Table 4).

Our comparative analysis highlights different trends of bone adaptation to a graviportal limb construction. Although some parameters were, for some bones, covarying with MD (size parameter), it was never the case for all bones (see Suppl. 1) -- hence all the selected parameters display signals that are not solely attributable to size or allometry.

Graviportal taxa are large animals with relatively larger cross-sections in their humeri, femora and ribs, reflecting greater resistance to compression and tension as well as greater bone mass, especially in the stylopodia. They are also characterized by a thicker cortex and a proportionally smaller medullary cavity, with a wider transition zone between the cortex and the medullary cavity, notably linked to the filling of the medullary area by a spongiosa with variations in trabecular thickness and size of intertrabecular spaces. This inner cancellous structure may add benefits for impact energy absorption and marrow support [11, 12]. Wall [15] noted the filling of the medullary cavity in *Ceratotherium*, suggesting a link with the animal's great weight, and the differences in the type of spongiosa between *Ceratotherium* and *Hippopotamus*. Our results also show that graviportal taxa exhibit higher values for the midshaft polar second moment of area, indicating increased resistance to stresses engendered by bending and torsion [30] that predominate in vertebrate limb bones during locomotion [31]. Results concerning the two stylopodial limb bones are strongly congruent.

However, rib microanatomical adaptation differs as summarized above. If there is a clear increase in bone mass in the ribs of some graviportal taxa, comparable to that observed in graviportal long bones, a similar phenomenon seems to occur for the bipedal forms sampled -- but conversely not for the rhinoceroses and mammoth. Our analyses thus showed an absence of significant signal in the rib MANOVA and a low K-NN classification power for this bone. Considering the difficulty of making homologous comparisons with ribs (see comments in [25, 32]), it appears necessary to increase taxon sampling and to analyse variations along the rib and the ribcage in various taxa (as in [33] for one sauropod) in order to better document and understand rib adaptations to changes of biomechanical constraints.

Distinguishing graviportal and amphibious adaptations

The variations we have detected among graviportal taxa are interesting—not all graviportal tetrapods converge on the same bone inner morphologies. Alexander and Pond [7] established that, although elephants, rhinoceroses and hippopotamus are considered graviportal taxa, elephants strongly differ from the two other groups in their relatively much longer legs (predominated by long stylopodia). The posture and gait of elephants is often mis-characterized as uniformly "columnar" and restricted to simply walking (see [34, 35]) but is nonetheless very distinct from rhinos and hippos in form and hence likely biomechanical function as well. Likewise, hippos are known only to trot on land, never gallop, whereas even large extant rhinos can gallop and elephants can or do not [7, 34], so biomechanical and

behavioural disparity exists even between these taxa. Such gross differences between these three groups of extant mammals are not evident at the microanatomical level (see "Qualitative analysis").

Despite this variability, a clear trend is observed across graviportal tetrapods examined here. The increase in bone mass (as represented by the infilling of marrow cavities and increased bone compactness; also see Christiansen, REF) observed in graviportal taxa, including the amphibious *Hippopotamus*, is more restricted compared to that observed in some other amniotes, especially some shallow water swimmers or bottom-walkers that are almost exclusively aquatic (see [20, 28, 29]). Adaptation to a graviportal morphology and related behaviours is thus not to be mistaken for the specialization of bone mass increase observed in these aquatic taxa.

However, it is difficult to determine if the pattern observed in *Hippopotamus* reflects its graviportal limbs or the benefit of a slight increase in bone mass in its legs in order to be used as ballast and to stabilize in water. As a result both adaptations might be mistaken, or even synergistic and pointless to try to untangle from their evolutionary integration. Adaptation to a graviportal limb morphology should thus be taken into consideration when analysing possibly amphibious taxa displaying a terrestrial-like morphology, and thus notably in the study of the early stages of adaptation to an aquatic life in amniotes. This cautionary note is particularly relevant for interpreting less well understood large extinct forms such as some south American endemic ungulates (AH, unpublished observations), some giant xenarthrans and marsupials, *Arsinoitherium* and related giant tethytheres (including basal Proboscidea), and the diversity of large and small Rhinocerotoidea (e.g., [34–36]).

Methods

Material

The material analysed consists of humeri, femora and ribs of a large sample of fossil and extant mammals and reptiles. The taxa were chosen based on availability (including good preservation of the bone mid-diaphysis and feasibility of obtaining good quality digital imaging data, in addition to general accessibility to our research team) with the aim of including large forms and of representing diverse postures and locomotor habits (e.g., terrestrial vs. aquatic) (see Tables 1-3; Fig. 1). Our final sample consisted of 54 humeri of 49 species, 43 femora of 38 species (and two indeterminate theropod dinosaurs; although their

phylogenetic position could not be determined precisely, so that they could not be incorporated in analyses taking the phylogeny into consideration, they could increase the sample of bipedal taxa), and 25 ribs of 25 species. Stylopodial bones were chosen because they are thought to have a stronger ecological signal than zeugopodial ones [26, 27] and show a much larger cross-sectional area in graviportal taxa ([7], REFS). Complete cross-sectional microanatomical data for stylopodial bones are rare for giant sauropods because of practical constraints imposed by the bone size. Conversely, whole transverse rib sections were available, which explains why ribs were also chosen for the analysis.

Bone section analysis

Some bones were sectioned using standard petrographic thin-section techniques (e.g. [37]; Tables 1-3). Others were scanned using high-resolution computed tomography (GEphoenix|X-ray v|tome|xs 240) at the Steinmann-Institut, University of Bonn (Germany) and at the AST-RX platform of the Muséum National d'Histoire naturelle (UMS 2700) or at the Equine Diagnostic Imaging Centre at the Royal Veterinary College (GE Lightspeed), with reconstructions performed using datox/res or similar software (e.g., in case of the GE Lightspeed scans, Medview software (www.Medimage.com)). Image segmentation and visualization were performed from the reconstructed image data using VGStudioMax 2.0 and 2.2 (Volume Graphics Inc., Heidelberg, Germany). These techniques have already been shown neither to introduce artefacts nor to bias interpretation of the results for comparative analyses [25, 38]. New virtual thin-sections were made from the microtomographic data in cross-sectional planes of interest that serve as references for our comparative studies. For long bones, these were diaphyseal transverse sections showing the thickest cortex, and thus assumed to cross the growth centre (see [39, 40]). Rib transverse sections were made at about the first third of the proximodistal distance along the rib's perimeter, which has been shown to be the location of the growth centre in ribs [33].

Scans of the classical (physical) thin-sections, performed at high resolution (i.e., between 6400 and 12800 dpi) using an Epson V750-M Pro scanner, and virtual thin-sections were transformed into single-bit digital images using Photoshop CS3 (where black represents bone and white cavities), and analysed using the software Bone Profiler [41]. Some additional sections, either histological thin sections or virtual thin sections, come from previous studies [20, 21, 42]. Quantitative parameters were measured directly on these images, again via Bone Profiler [41] but also via the ImageJ plugin BoneJ [43], except for maximal bone diameter (MD), which was taken directly from the sections. These parameters included (see [41] for

details and illustrations): (1) C: compactness of the whole section (i.e., surface occupied by bone divided by whole sectional area); (2) P: the extent of the medullary cavity as measured by the relative distance from the centre of the section to the point where the most abrupt change in compactness occurs; (3) S: the width of the transitional zone between the compact cortex and the medullary cavity as measured by the reciprocal of the slope of the compactness profile at the inflection point; (4) MD: maximum bone diameter at the level of section (here considered as a proxy for body size); (5) R/t: outside radius of the bone divided by the thickness of the cortex ([44]); (6) CSS: cross-sectional shape ($=I_{max}/I_{min}$; the ratio of maximal to minimal second moments of area); (8) J: polar second moment of area ($=I_{max} + I_{min}$); (9) Z_{pol}: polar section modulus (see for definitions of these measurements #6-9 and usage in BoneJ software); and (10) Per: perimeter of the section.

Statistical analyses

All data were $\log_{10}$ transformed prior to analyses (CSA and Z_{pol} were first raised to the power of 0.50 and 0.33, respectively, reducing them to dimensions more comparable to linear values) to meet assumptions of normality and homoscedasticity required for parametric analyses. Considering that the parameter maximal diameter (MD) is usually considered as an estimate of overall body size [41], and actual body mass data were not available for our specimens, we performed linear regression analyses on the various microanatomical parameters in order to evaluate the scaling of each parameter vs. MD in the dataset. Because of the very strong impact of MD on the parameters Per, CSA and Zpol (r~0.99), the later were removed from the analyses, to avoid multiplying the same signal. The amount of phylogenetic signal was investigated for the different parameters analysed, as follows. Statistical tests were performed using an approximate "consensus" phylogeny, derived from several published phylogenies [45–52] (Fig.7). We calculated the K-statistic following Blomberg, Garland & Ives [53], which compares the observed phylogenetic signal in a trait to the signal under a Brownian motion model of trait evolution. Species means were used when several specimens were available for the same species. A K-value lower than one implies less similarity between relatives than expected under Brownian motion. We then performed linear regression analyses on all parameters in order to evaluate the allometry in the data. As a phylogenetic signal generally was detected, we calculated independent contrasts and forced regressions through the origin. We then conducted a Principal Components Analysis (PCA) in order to explore the distribution of the different taxa in morphospace. Four groups were defined based on their typical limb posture and locomotor habit: (1) Graviportal (i.e., with robust bones with

relatively long stylopodia; likely columnar posture), (2) Quadrupedal (graviportal taxa excluded), (3) Bipedal and (4) Aquatic (groups 1-3 being predominantly terrestrial taxa). In order to clearly visualize the trends between the different groups, a between-groups PCA was performed (on the mean values for each group). We also performed a pattern recognition analysis using the K-nearest neighbours algorithm (see [54]) in order to discriminate between our groups while avoiding possible biases linked to more classical discriminant analyses (notably as a result of the small number of specimens for some groups). Phylogenetic ANOVAs and ANCOVAs (when a size effect was detected), as well as phylogenetic MANOVAS were performed as tests to determine if the group number had a significant correlation with the various parameters analysed.

All statistical analyses were performed using the statistical software R [55] except phylogenetic ANCOVAs that required the use of the PDSIMUL and PDANOVA routines implemented in PDAP [56]. In the PDSIMUL program, we used Brownian motion as our model for evolutionary change and ran 1000 unbounded simulations to create an empirical null distribution against which the F-values from the original data could be compared.

Competing interests

The authors declare that they have no competing interests

Authors' contributions

AH designed the study. AH, KW, SH, AHL and JRH participated to the data acquisition. AH conducted the analyses and drafted the manuscript, with significant inputs from RC and JRH, respectively. All authors contributed to the final manuscript, read it and approved it.

Acknowledgments

We warmly thank O. Dülfer, P. Göddertz, Y. Nakajima, P.M. Sander, R. Schellhorn and J. Schultz, (Steinmann-Institut, University of Bonn, Bonn, Germany), C. Bens and J. Lesur (Muséum National d'Histoire naturelle, Paris, France), N. Klein (Staatliches Museum für Naturkunde, Stuttgart, Germany), O. Mateus (Museu da Lourinha, Lourinha , Portugal), R. Scheetz (Brigham Young University, Utah, USA), W. Simpson (Field Museum of Natural History, Chicago, USA), F. Straehl, T. Scheyer and M. Sanchez-Villagra (Universität Zurich, Zurich, Switzerland), R. Barsbold, K. Tsogtbaatar and C. Tsogtbaatar (Mongolian Paleontological Center, Ulaanbaatar, Mongolia), D. Brinkman and M. Fox (Yale Peabody

Museum, Yale University, New Haven, USA), S. Ishigaki, M. Saneyoshi and S. Suzuki (Hayashibara Museum of Natural Sciences, Okayama, Japan), H. Taruno (Osaka Museum of Natural History, Osaka, Japan), T. Ando, H. Sawamura and T. Shinmura (Ashoro Museum of Paleontology, Ashoro, Japan), S. Kawada, M. Manabe, R. Miyawaki, R. Tajiri and T. Yamada (National Science Museum, Tokyo, Japan), Y. Kobayashi, K. Nakamura and H. Nomura (Hokkaido University, Sapporo, Japan), H. Berke (Universität Köln, Köln, Germany), K. Padian and S. Werning (University of California Museum of Paleontology, Barkley, USA), R. Irmis (Utah Musum of Natural History, Utah, USA), T. Bolliger and H.J. Siber (Sauriermuseum Aathal, Switzerland), G.W. Storrs (Cincinnati Museum Center, Ohio, USA), M. Lowe (University Museum of Zoology, Cambridge) and R. Sabin (Natural History Museum, Department of Zoology, London) for the loan of specimens, sections or images. Input on earlier, independent inceptions of this study from S. Shefelbine, M. Doube, M. Laurin and S. Pierce is appreciated. We thank the Steinmann Institut (University of Bonn, Germany) for providing beamtime and support, UMS 2700 outils et méthodes de la systématique intégrative CNRS-MNHN and AST-RX, Plateau technique d'accès scientifique à la tomographie à rayons X du MNHN, M. Garcia Sanz for performing the scans and reconstructions at the AST-RX platform (MNHN, Paris, France), and UMR 7207 CR2P MNHN CNRS UPMC-Paris6 for 3D imaging facilities. A.H. thanks F. Goussard (MNHN, Paris, France) for discussions about graviportality and A.C. Fabre (Duke University, NC, USA) for her help with statistics. A.H. acknowledges financial support from the ANR-13-PDOC-001 and the A. v. Humboldt Foundation. J.R.H. was funded by grants from the Natural Environment Research Council (UK). Funding was provided by the Japanese Society for the Promotion of Science (JSPS) to S.H.

References

1. Gray J. Animal Locomotion. Lond Weidenfield Nicolson; 1968.

2. Polly PD, Hall B. Limbs in mammalian evolution. Fins Limbs Evol Dev Transform; 2007. p. 245-268.

3. Hildebrand M. Analysis of vertebrate structure; 1982.

4. Carrano MT. The evolution of dinosaur locomotion: functional morphology, biomechanics, and modern analogs; 1998.

5. Ramsay EC, Henry RW, Csuti B, Sargent E, Bechert U. Anatomy of the elephant foot. Elephants Foot Prev Care Foot Cond Captive Asian Afr Elephants. 2001:9-12.

6. Gregory WK. Notes on the principles of quadrupedal locomotion and on the mechanism of he limbs in hoofed animals. Ann N Y Acad Sci. 1912:22:267-294.

7. Alexander R, Pond C. Locomotion and bone strength of the white rhinoceros, *Ceratotherium simum*. J Zool. 1992:227:63-69.

8. Schmidt-Nielsen K. Scaling: Why Is Animal Size so Important? Cambridge University Press; 1984.

9. Ross MD. The influence of gravity on structure and function of animals. Adv Space Res. 1984:4:305–314.

10. Doube M, Kłosowski MM, Wiktorowicz-Conroy AM, Hutchinson JR, Shefelbine SJ: Trabecular bone scales allometrically in mammals and birds. Proc R Soc B Biol Sci. 2011: 278:3067-3073.

11. Oxnard CE. Bone and bones, architecture and stress, fossils and osteoporosis. J Biomech. 1993:26:63-79.

12. Oxnard C. From giant ground sloths to human osteoporosis: an essay on the architecture and biomechanics of bone. 1990:3:75-96.

13. Sander PM, Christian A, Clauss M, Fechner R, Gee CT, Griebeler E-M, Gunga H-C, Hummel J, Mallison H, Perry SF, Preuschoft H, Rauhut OWM, Remes K, Tütken T, Wings O, Witzel U. Biology of the sauropod dinosaurs: the evolution of gigantism. Biol Rev. 2011: 86:117-155.

14. Houssaye A. “Pachyostosis” in aquatic amniotes: a review. Integr Zool. 2009:4:325-340.

15. Wall WP. The correlation between high limb-bone density and aquatic habits in recent mammals. J Paleontol. 1983:57:197-207.

16. Fish FE, Stein BR. Functional correlates of differences in bone density among terrestrial and aquatic genera in the family Mustelidae (Mammalia). *Zoomorphology* 1991, 110:339–345.

17. De Buffrénil V, Canoville A, D’Anastasio R, Domning DP: Evolution of sirenian pachyosteosclerosis, a model-case for the study of bone structure in aquatic tetrapods. J Mamm Evol. 2010:17:101-120.

18. Clementz MT, Holroyd PA, Koch PL. Identifying aquatic habits of herbivorous mammals through stable isotope analysis. Palaios. 2008:23:574-585.

19. Cubo J, Ponton F, Laurin M, Margerie E de, Castanet J. Phylogenetic signal in bone microstructure of sauropsids. Syst Biol. 2005:54:562-574.

20. Hayashi S, Houssaye A, Nakajima Y, Chiba K, Ando T, Sawamura H, Inuzuka N, Kaneko N, Osaki T: Bone inner structure suggests increasing aquatic adaptations in Desmostylia (Mammalia, Afrotheria). PLoS ONE. 2013:8:e59146.

21. Straehl FR, Scheyer TM, Forasiepi AM, MacPhee RD, Sánchez-Villagra MR. Evolutionary patterns of bone histology and bone compactness in xenarthran mammal long bones. PLoS ONE. 2013:8:e69275.

22. Amson E, Argot C, McDonald HG, de Muizon C. Osteology and functional morphology of the forelimb of the marine sloth *Thalassocnus* (Mammalia, Tardigrada). J Mamm Evol. 2014.

23. Garland Jr T. Phylogenetic comparison and artificial selection. In *Hypoxia*. Springer; 2001:107-132.

24. Carrano MT. Implications of limb bone scaling, curvature and eccentricity in mammals and non-avian dinosaurs. *J Zool.* 2001:254:41-55.

25. Houssaye A, Tafforeau P, Herrel A. Amniote vertebral microanatomy–what are the major trends? *Biol J Linn Soc.* 2014:112:735-746.

26. Canoville A, Laurin M. Evolution of humeral microanatomy and lifestyle in amniotes, and some comments on palaeobiological inferences. *Biol J Linn Soc.* 2010:100:384-406.

27. Quemeneur S, Buffrénil V, Laurin M. Microanatomy of the amniote femur and inference of lifestyle in limbed vertebrates. *Biol J Linn Soc.* 2013:109:644-655.

28. Houssaye A, Lindgren J, Pellegrini R, Lee AH, Germain D, Polcyn MJ. Microanatomical and histological features in the long bones of mosasaurine mosasaurs (Reptilia, Squamata) - Implications for aquatic adaptation and growth rates. PLoS ONE. 2013:8:e76741.

29. Klein N, Houssaye A, Neenan JM, Scheyer TM. Long bone histology and microanatomy of Placodontia (Diapsida: Sauropterygia). Contrib Zool. 2015:84:59-84.

30. O'Neill MC, Ruff CB. Estimating human long bone cross-sectional geometric properties: a comparison of noninvasive methods. J Hum Evol. 2004:47:221-235.

31. Ruff CB. Long bone articular and diaphyseal structure in old world monkeys and apes. I: locomotor effects. Am J Phys Anthr. 2002:119:305-42.

32. Houssaye A, Bardet N. Rib and vertebral micro-anatomical characteristics of hydropelvic mosasauroids. Lethaia 2012:45:200:209.

33. Waskow K, Sander PM. Growth record and histological variation in the dorsal ribs of *Camarasaurus* sp. (Sauropoda). J Vertebr Paleontol. 2014:34:852-869.

34. Gheerbrant E, Tassy P. L'origine et l'évolution des éléphants. Comptes Rendus Palevol. 2009:8:281-294.

35. Antoine P-O, Ducrocq S, Marivaux L, Chaimanee Y, Crochet J-Y, Jaeger J-J, Welcomme J-L. Early rhinocerotids (Mammalia: Perissodactyla) from South Asia and a review of the Holarctic Paleogene rhinocerotid record. Can J Earth Sci. 2003. 40:365-374.

36. Vizcaino SF, Cassini GH, Toledo N, Bargo MS. On the evolution of large size in mammalian herbivores of Cenozoic. Bones Clones Biomes Hist Geogr Recent Neotropical Mamm. 2012:76.

37. Houssaye A, Buffrenil V de, Rage JC, Bardet N. An analysis of vertebral “pachyostosis” in *Carentonosaurus mineaui* (Mosasauroidea, Squamata) from the Cenomanian (early Late Cretaceous) of France, with comments on its phylogenetic and functional significance. J Vertebr Paleontol 2008:28:685-691.

38. Dumont M, Laurin M, Jacques F, Pelle E, Dabin W, de Buffrenil V. Inner architecture of vertebral centra in terrestrial and aquatic mammals: a two-dimensional comparative study. J Morphol 2013:274:570-84.

39. Houssaye A, Scheyer TM, Kolb C, Fischer V, Sander PM: A new look at ichthyosaur long bone microanatomy and histology: Implications for their adaptation to an aquatic life. PLoS ONE. 2014:9:e95637.

40. Nakajima Y, Hirayama R, Endo H. Turtle humeral microanatomy and its relationship to lifestyle. Biol J Linn Soc. 2014:112:719-734.

41. Girondot M, Laurin M: Bone profiler: a tool to quantify, model, and statistically compare bone-section compactness profiles. J Vertebr Paleontol. 2003:23:458-461.

42. Laurin M, Canoville A, Germain D. Bone microanatomy and lifestyle: A descriptive approach. Comptes Rendus Palevol. 2011:10:381-402.

43. Doube M, Kłosowski MM, Arganda-Carreras I, Cordelières FP, Dougherty RP, Jackson JS, Schmid B, Hutchinson JR, Shefelbine SJ: BoneJ: Free and extensible bone image analysis in ImageJ. Bone 2010:47:1076-1079.

44. Currey JD, Alexander RM. The thickness of the walls of tubular bones. J Zool Lond. 1985:206:453-468.

45. Sereno PC: The evolution of dinosaurs. Science. 1999:284:2137-2147.

46. Gilbert C, Ropiquet A, Hassanin A. Mitochondrial and nuclear phylogenies of Cervidae (Mammalia, Ruminantia): Systematics, morphology, and biogeography. Mol Phylogenet Evol. 2006:40:101-17.

47. Remes K. Taxonomy of Late Jurassic diplodocid sauropods from Tendaguru (Tanzania). Foss Rec. 2009:12:23-46.

48. Todd NE. New phylogenetic analysis of the family elephantidae based on cranial-dental morphology. Anat Rec Hoboken. 2010:293:74-90.

49. Meredith RW, Janečka JE, Gatesy J, Ryder OA, Fisher CA, Teeling EC, Goodbla A, Eizirik E, Simão TL, Stadler T: Impacts of the Cretaceous Terrestrial Revolution and KPg extinction on mammal diversification. Science 2011:334:521-524.

50. Steiner CC, Ryder OA. Molecular phylogeny and evolution of the Perissodactyla. Zool J Linn Soc. 2011:163:1289-1303.

51. Bibi F: A multi-calibrated mitochondrial phylogeny of extant Bovidae (Artiodactyla, Ruminantia) and the importance of the fossil record to systematics. BMC Evol Biol. 2013, 13:166.

52. Thompson RS, Parish JC, Maidment SC, Barrett PM: Phylogeny of the ankylosaurian dinosaurs (Ornithischia: Thyreophora). J Syst Palaeontol. 2012:10:301-312.

53. Blomberg SP, Garland T, Ives AR. Testing for phylogenetic signal in comparative data: behavioral traits are more labile. Evolution. 2003:57:717-745.

54. Cornette R, Herrel A, Stoetzel E, Moulin S, Hutterer R, Denys C, Baylac M. Specific information levels in relation to fragmentation patterns of shrew mandibles: do fragments tell the same story? J Archaeol Sci. 2015:53:323-330.

55. Team RC. R: A language and environment for statistical computing. R Foundation for Statistical Computing, Vienna, Austria, 2012.

56. Garland T, Dickerman AW, Janis CM, Jones JA. Phylogenetic analysis of covariance by computer simulation. Syst Biol. 1993:42:265-292.

Figure legends

Figure 1. Schematic drawings illustrating the diversity of microanatomical patterns observed in humeri of: A- *Giraffa camelopardalis*, B- *Choeropsis liberiensis*, C- *Hippopotamus amphibious*, D- *Ampelosaurus atacis*, E- *Centrosaurus apertus*, F- *Ceratotherium simum*, G- *Rhinoceros unicornis*, H- *Elephas maximus*, I- *Diceros bicornis*, J- *Trichechus manatus*, K- *Paleoparadoxia sp.*, L- *Dugong dugon*. Scale bars: 5 mm.

Figure 2. Schematic drawings illustrating the diversity of microanatomical patterns observed in femora of: A- *Giraffa camelopardalis*; B- *Syncerus caffer*, C- *Rhinoceros unicornis*, D- *Rhinoceros sondaicus*, E- *Elephas maximus*, F- *Mammuthus* sp., G- *Hippopotamus amphibious*, H- *Stegosaurus* sp. Scale bars: 5 mm

Figure 3. Schematic drawings illustrating the diversity of microanatomical patterns observed in ribs of: A- *Martes foina*, B- *Ursus spelaeus*, C- *Paleoparadoxia sp.*, D- *Miragaia longicollum*, E- *Cathetosaurus* sp., F- *Lourinhanosaurus* sp., G- *Baryonyx* sp., H- *Mammuthus primigenius*, I- *Rhinoceros unicornis.* Scale bars: 5 mm (except for *Martes*: 0.5 mm).

Figure 4. Microanatomical clusters obtained by Principal Component Analyses (PCA) conducted on the humeri of our sample. Graphs showing the distribution of the variance in all taxa examined according to the PCA1 and PCA2 axes. A, classical PCA; B, between-groups PCA. Abbreviations for the taxa in the PCA graphs as in Table 1.

Figure 5. Microanatomical clusters obtained by Principal Component Analyses (PCA) conducted on the femora of our sample. Graphs showing the distribution of the variance in all taxa examined according to the PCA1 and PCA2 axes. A, classical PCA; B, between-groups PCA. Abbreviations for the taxa in the PCA graphs as in Table 2.

Figure 6. Microanatomical clusters obtained by Principal Component Analyses (PCA) conducted on the ribs of our sample. Graphs showing the distribution of the variance in all taxa examined according to the PCA1 and PCA2 axes. A, classical PCA; B, between-groups PCA. Abbreviations for the taxa in the PCA graphs as in Table 3.

Figure 7. Consensus phylogenetic tree (based on [45–52]) with the 4 groups defined in the present study illustrated (yellow: graviportal; green: quadrupedal (graviportal taxa excluded); orange: bipedal; blue: aquatic).

Table 1. List of the humeri analyzed in this study. Abb: abbreviations; P: posture; G: graviportal; B: bipedal; Q: quadrupedal; A: aquatic; ST: section type; CS: classical section; VS: virtual section.

Family	Taxon	Abb.	P	Coll Nb	ST
Diplodocidae	cf. *Apatosaurus sp.*	Ap	G	OMNH 01275	CS
Titanosauria	*Ampelosaurus atacis*	Am	G	MDE C3-270	CS
Tyrannosauridae	*Tarbosaurus sp.*	Tar	B	HMNS 94-10-78	CS
Allosauridae	*Allosaurus fragilis*	All	B	UMNH 3607	CS
Stegosauria	*Scutellosaurus lawleri*	Sc	B	UCMP 13068	CS
	Scutellosaurus lawleri	Sc	B	UCMP 130580	CS
Protoceratopsidae	*Protoceratops andrewsi*	Pr	G	MPC-D 100/530	CS (2)
	Centrosaurus apertus	Cen	G	RTMP 79.14.759	CS
Nothrotheriidae	*Nothrotherium escrivanse*	No	Q	PIMUZ A/V 477	Straehl et al. (2013)
Myrmecophagidae	*Tamandua tetradactyla*	Tam	Q	NMB 10420	Straehl et al. (2013)
	Myrmecophaga tridactyla	My	Q	ZMZ 11119	Straehl et al. (2013)
Desmostylia	*Paleoparadoxia sp.*	Pal	A	AMP AK0011	CS
Trichechidae	*Trichechus manatus*	Tr	A	NSM M 34694	VS
Stegodontidae	*Stegodon aurorae*	St	G	OMNH QV 264	CS
Elephantidae	*Elephas maximus*	El	G	JRHRVC uncat.	VS
Elephantidae	*Loxodonta africana*	Lo	G	NHMUK 1939.5.27.1	VS
Felidae	*Felis felis*	Fe	Q	UFGK uncat.	VS
Felidae	*Panthera leo*	Pa	Q	MNHN1912-398	Laurin et al. 2011
Felidae	*Uncia uncia*	Un	Q	NSM M 33876	VS
Canidae	*Canis lupus*	Ca	Q	Unnumbered	Laurin et al. 2011
Canidae	*Vulpes vulpes*	Vu	Q	STIPB M12	VS
Mustelidae	*Meles meles*	Me	Q	STIPB M4002	VS
Ursidae	*Ursus thibetanus*	Ut	Q	ZFMK 81557	VS
	Ursus maritimus	Um	Q	ZFMK 2005.356	VS
Equidae	*Equus burchelli*	Eq	Q	NMW 28810	Laurin et al. 2011
Tapiridae	*Tapirus terrestris*	Tap	Q	ZFMK 462	VS
Rhinocerotidae	*Diceratherium sp.*	Dic	G	NHMUK PV M7752	VS
Rhinocerotidae	*Diceros bicornis*	Db	G	UMZC H.6481	VS

Rhinocerotidae	*Diceros bicornis*	Db	G	NHMUK M92402	VS
Rhinocerotidae	*Ceratotherium simum*	Ce	G	JRHRVC uncat.	VS
	Ceratotherium simum	Ce	G	MNHN ZM MO 2005-297	VS
Rhinocerotidae	*Dicerorhinus sumatrensis*	Di	G	UMZC H.6392	VS
	Dicerorhinus sumatrensis	Di	G	MNHN ZM AC 1903-300	VS
	Rhinoceros sondaicus	Rs	G	MNHN ZM AC A7970	VS
	Rhinoceros unicornis	Ru	G	MNHN ZM AC 1960-59	VS
Hippopotamidae	*Choeropsis liberiensis*	Ch	G	ZFMK 65 570	VS
Hippopotamidae	*Hippopotamus amphibius*	Hi	G	UMZC H.10714	VS
Suidae	*Sus scrofa*	Su	Q	STIPB M56	VS
Giraffidae	*Giraffa camelopardalis*	Gi	Q	JRHRVC uncat.	VS
Giraffidae	*Okapia johnstoni*	Ok	Q	UMZC H.20302	VS
Cervidae	*Rangifer tarandus*	Ra	Q	STIPB M47	VS
	Capreolus capreolus	Cp	Q	MNHN CH 221	Laurin et al. 2011
	Alces americanus	Al	Q	UMZC H.17691	VS
	Cervus elaphus	Cer	Q	MNHN Unnumbered	Laurin et al. 2011
Cervidae	*Megaloceros sp.*	Meg	Q	UCMP 63524	VS
Cervidae	*Megaloceros giganteus*	Meg	Q	UMZC H.17535	VS
	Dama dama	Da	Q	STIPB M1	VS
Bovidae	*Cephalophus sylvicultor*	Cep	Q	NHMUK ZD 1961.8.9.80-1	VS
Bovidae	*Ovis ammon*	Ov	Q	NMW 26499	Laurin et al. 2011
Bovidae	*Rupicapra*	Rup	Q	STIPB M1639	VS
	Capra falconeri	Cap	Q	NMW 12081	Laurin et al. 2011
Bovidae	*Boselaphus tragocamelus*	Bo	Q	NMW 25399	Laurin et al. 2011
Bovidae	*Taurotragus oryx*	Tau	Q	NMW 61319	Laurin et al. 2011
Bovidae	*Syncerus caffer*	Sy	Q	NHMUK ZD 1874.11.2.4	VS

Family	Taxon	Abb.	P	Coll Nb	ST
Ornithomimidae	*Gallimimus* sp.	Ga	B	HMNS 97-21-378	CS
Allosauridae	*Allosaurus fragilis*	All	B	UMNH 3694	CS
Abelisauridae	*Masiakasaurus knopfleri*	Ma	B	FMNH PR 2123	CS
Theropoda	Theropod indet.	Th	B	HMNS 2006-04-356	CS
Theropoda	Theropod indet.	Th	B	HMNS 2006-04-151	CS
Hypsilophodontidae	*Dryosaurus altus*	Dr	B	BYU 13312	CS
Stegosauria	*Scutellosaurus lawleri*	Sc	B	UCMP 170829	CS
Stegosauridae	*Stegosaurus* sp.	St	G	YPM 4634	CS
Myrmecophagidae	*Myrmecophaga tridactyla*	My	Q	ZMZ 11119	Straehl et al. (2013)
Myrmecophagidae	*Tamandua tetradactyla*	Tam	Q	NMB 10420	Straehl et al. (2013)
Elephantidae	*Mammuthus* sp.	Ma	G	UCMP 35984	VS
Elephantidae	*Mammuthus* sp.	Ma	G	NHMUK uncat.	VS
Elephantidae	*Elephas maximus*	El	G	JRHRVC uncat.	VS
Elephantidae	*Loxodonta africana*	Lo	G	NHMUK 1939.5.27.1	VS
Felidae	*Felis felis*	Fe	Q	UFGK uncat.	VS
Felidae	*Uncia uncia*	Un	Q	NSM M 33876	VS
Canidae	*Vulpes vulpes*	Vu	Q	STIPB M12	VS
Mustelidae	*Meles meles*	Me	Q	STIPB M4002	VS
Ursidae	*Ursus thibetanus*	Ut	Q	ZFMK 81557	VS

Table 2. List of the femora analyzed in this study. Abb: abbreviations; P: posture; G: graviportal; B: bipedal; Q: quadrupedal; A: aquatic; ST: section type; CS: classical section; V: virtual section.

	Ursus maritimus	Um	Q	ZFMK 2005.356	VS
Tapiridae	*Tapirus terrestris*	Ta	Q	ZFMK 462	VS
Rhinocerotidae	*Ceratotherium simum*	Ce	G	MNHN ZM MO 2005-297	VS
	Ceratotherium simum	Ce	G	JRHRVC uncat.	VS
	Dicerorhinus sumatrensis	Di	G	MNHN ZM AC 1903-329	VS
	Rhinoceros sondaicus	Rs	G	MNHN ZM AC A7970	VS
	Rhinoceros unicornis	Ru	G	MNHN ZM AC 1960-59	VS
Hippopotamidae	*Choeropsis liberiensis*	Ch	Q	ZFMK 65 570	VS
Hippopotamidae	*Hippopotamus amphibius*	Hi	G	UMZC H.10714	VS
Camelidae	*Lama guanicoe*	La	Q	STIPB M7388	VS
Suidae	*Sus scrofa*	Su	Q	STIPB M56	VS
Giraffidae	*Okapia johnstoni*	Ok	Q	UMZC H.20302	VS
Giraffidae	*Giraffa camelopardalis*	Gi	Q	JRHRVC uncat.	VS
Cervidae	*Dama dama*	Da	Q	STIPB M1	VS
Cervidae	*Megaloceros sp.*	Meg	Q	UCMP 63524	VS
Cervidae	*Rangifer tarandus*	Ra	Q	STIPB M47	VS
	Capreolus capreolus	Cp		STIPB M1452	VS
Cervidae	*Alces americanus*	Al	Q	UMZC H.17691	VS
Bovidae	*Cephalophus sylvicultor*	Cep	Q	NHMUK ZD 1961.8.9.80-1	VS
Bovidae	*Rupicapra*	Ru	Q	STIPB M1639	VS
Bovidae	*Syncerus caffer*	Sy	Q	NHMUK ZD 1874.11.2.4	VS
Bovidae	*Bos taurus*	Bos	Q	NHMUK 47	VS
Bovidae	*Bison bonasus*	Bi	Q	ZFMK 2010-303	VS

Table 3. List of the ribs analyzed in this study. Abb: Abbreviations; P: posture; G: graviportal; B: bipedal; Q: quadrupedal; A: aquatic; ST: section type; CS: classical section; V: virtual section.

Family	Taxon	Abb.	P	Coll Nb	ST
Spinosauridae	*Baryonyx* sp.	Ba	B	ML 1190.7c	C
Sinraptoridae	*Lourinhanosaurus* sp.	Lou	B	ML 370C	C
Sauropoda	*Spinophorosaurus nigeriensis*	Sp	G	Ni5.40-7ax	C
Diplodocidae	*Apatosaurus* sp.	Ap	G	BYU 145	C
Diplodocidae	*Diplodocus* sp.	Di	G	CMC 9932	C
Camarasauridae	*Cathetosaurus* sp.	Ca	G	SMA 0002	C
Brachiosauridae	*Brachiosaurus* sp.	Br	G	FMNH 25107	C
Camptosauridae	*Draconyx* sp.	Dr	B	ML 439	C
Ankylosauridae	*Ankylosaurus indet*	An	G	HMNS 94-10-7	C
Stegosauridae	*Miragaia* sp.	Mi	G	ML 433A	C
Stegosauridae	*Hesperosaurus mjosi*	He	G	HMNS 014	C
Procaviidae	*Procavia capensis*	Pr	Q	NSM M 3497	V
Desmostylidae	*Behemotops katsuiei*	Be	A	AMP 22	C
Desmostylidae	*Paleoparadoxia sp.*	Pa	A	AMP AK1001	C
Elephantidae	*Mammuthus primigenius*	Ma	G	ZFMK 98 395	V
Mustelidae	*Martes foina*	Mar	Q	STIPB M4004	V
Ursidae	*Tremarctos ornatus*	Tr	Q	ZFMK 97.275	V
	Ursus spelaeus	Us	Q	xxx	V
	Ursus maritimus	Um	Q	ZFMK 2005.356	V
Tapiridae	*Tapirus terrestris*	Ta	Q	ZFMK 462	V
	Rhinoceros sondaicus	Rs	G	MNHN ZM AC A7970	V
	Rhinoceros unicornis	Ru	G	MNHN ZM AC 1960-59	V

Hippopotamidae	*Choeropsis liberiensis*	Ch	Q	ZFMK 65 570	V
Bovidae	*Bison bonasus*	Bi	Q	ZFMK 2010-303	V
	Capra aegagrus	Cap	Q	UFGK Uncat.	

Table 4. Table showing the F and p values obtained for the various analyses of (co)variance. In bold when p<0.05.

	Phylogenetic ANOVA		**ANCOVA**		**Phylogenetic ANCOVA**	
	F	**p**	**F**	**p**	**F**	**p**
HUMERUS						
C	**11.96**	**0.032**				
S			**5.49**	**0.024**	8.68	0.235
P	**14.16**	**0.015**				
RT	8.52	0.081				
CSS	1.14	0.794				
J			**5.28**	**0.026**	8.58	0.261
FEMUR						
C			**7.96**	**0.008**	8.84	0.105
S	4.86	0.412				
P			**7.99**	**0.008**	8.78	0.089
RT			**5.52**	**0.025**	8.77	0.212
CSS			**7.63**	**0.009**	9.00	0.103
J			**8.54**	**0.006**	9.05	0.081
RIB						
C	2.35	0.546				
S	2.44	0.529				
P	7.17	0.111				
RT	4.87	0.216				
CSS	0.77	0.852				
J			4.18	0.053	8.56	0.198

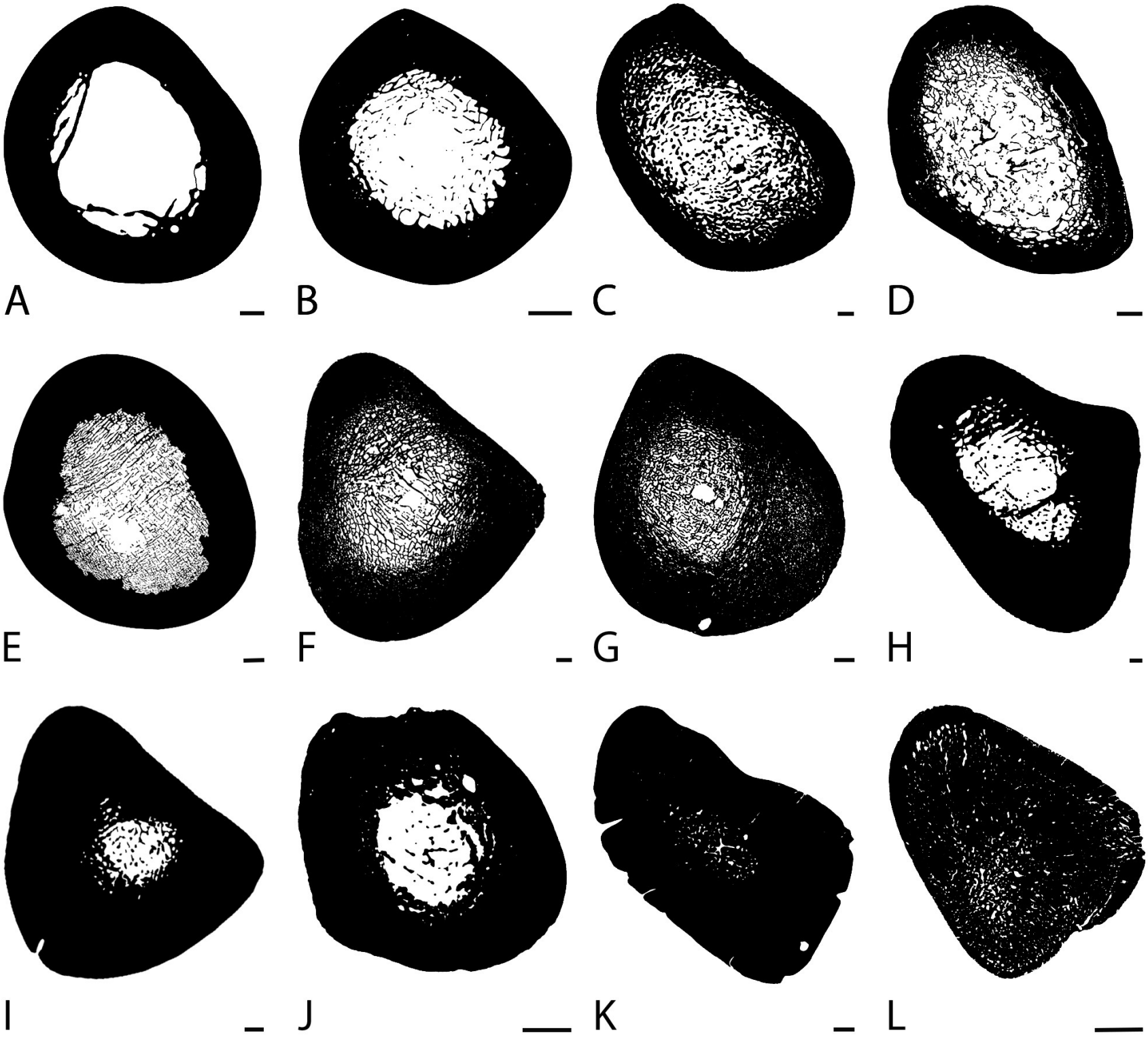
A
B
C
D
E
F
G
H
I
J
K
L

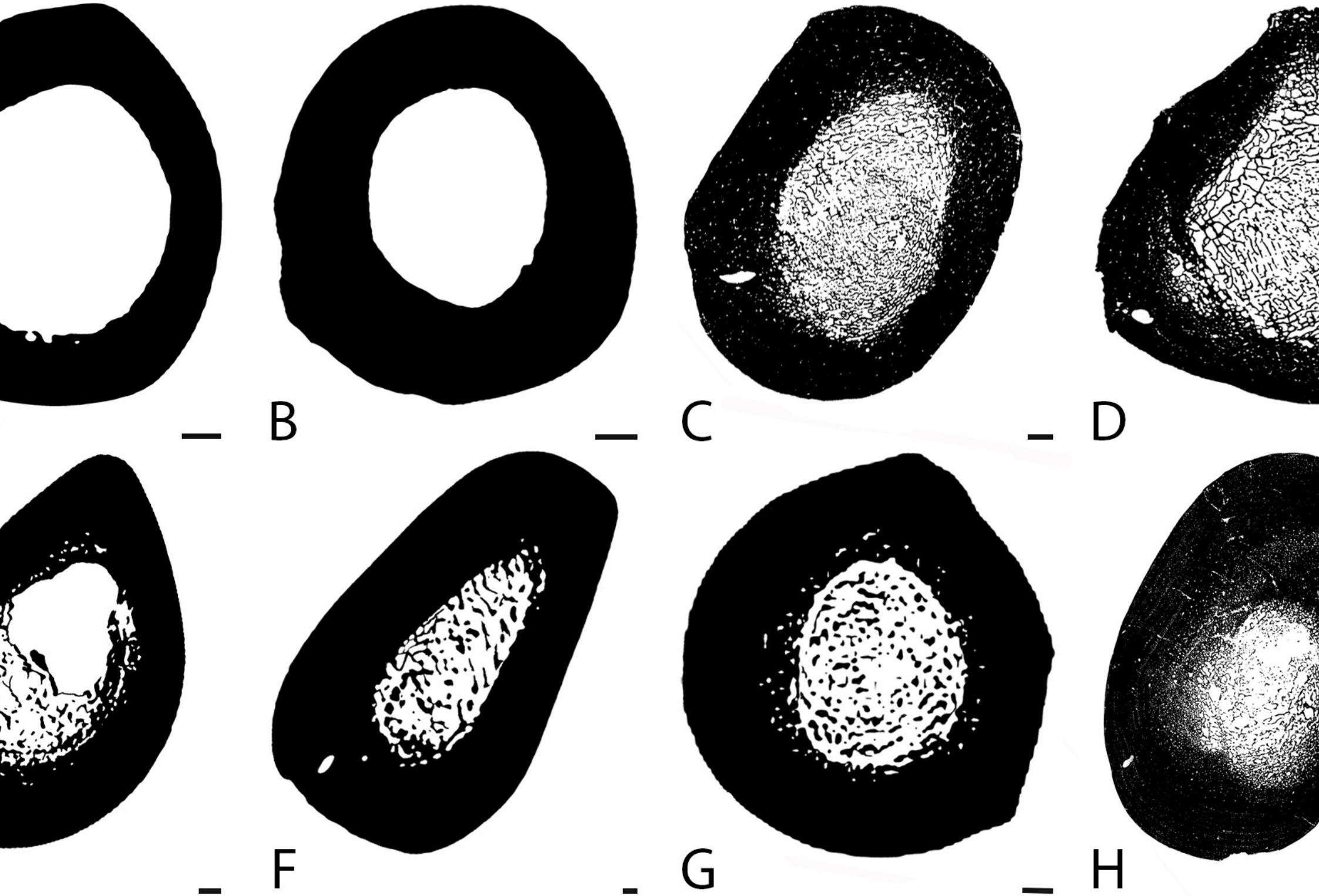
B
C
D
F
G
H

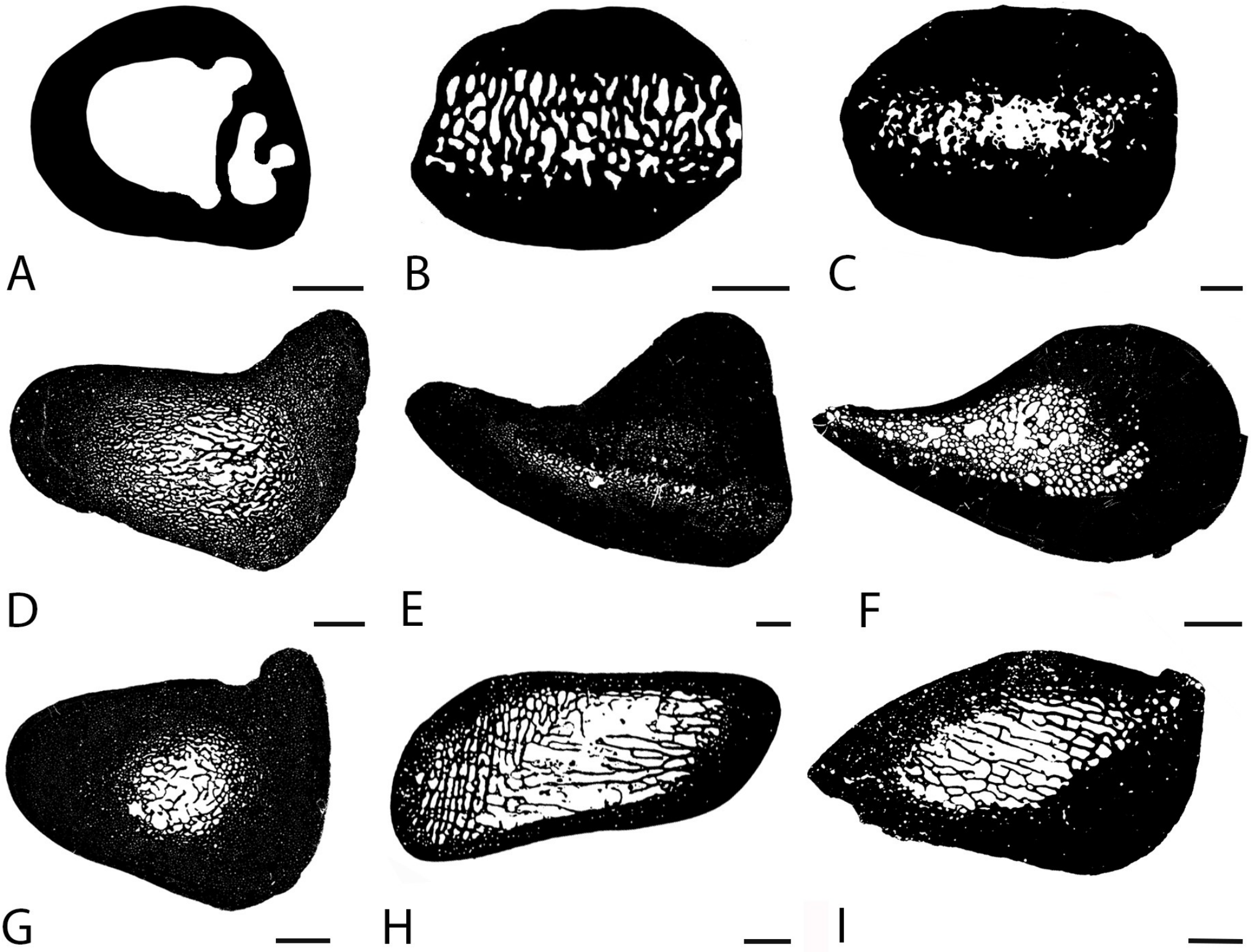
A
B
C
D
E
F
G
H
I

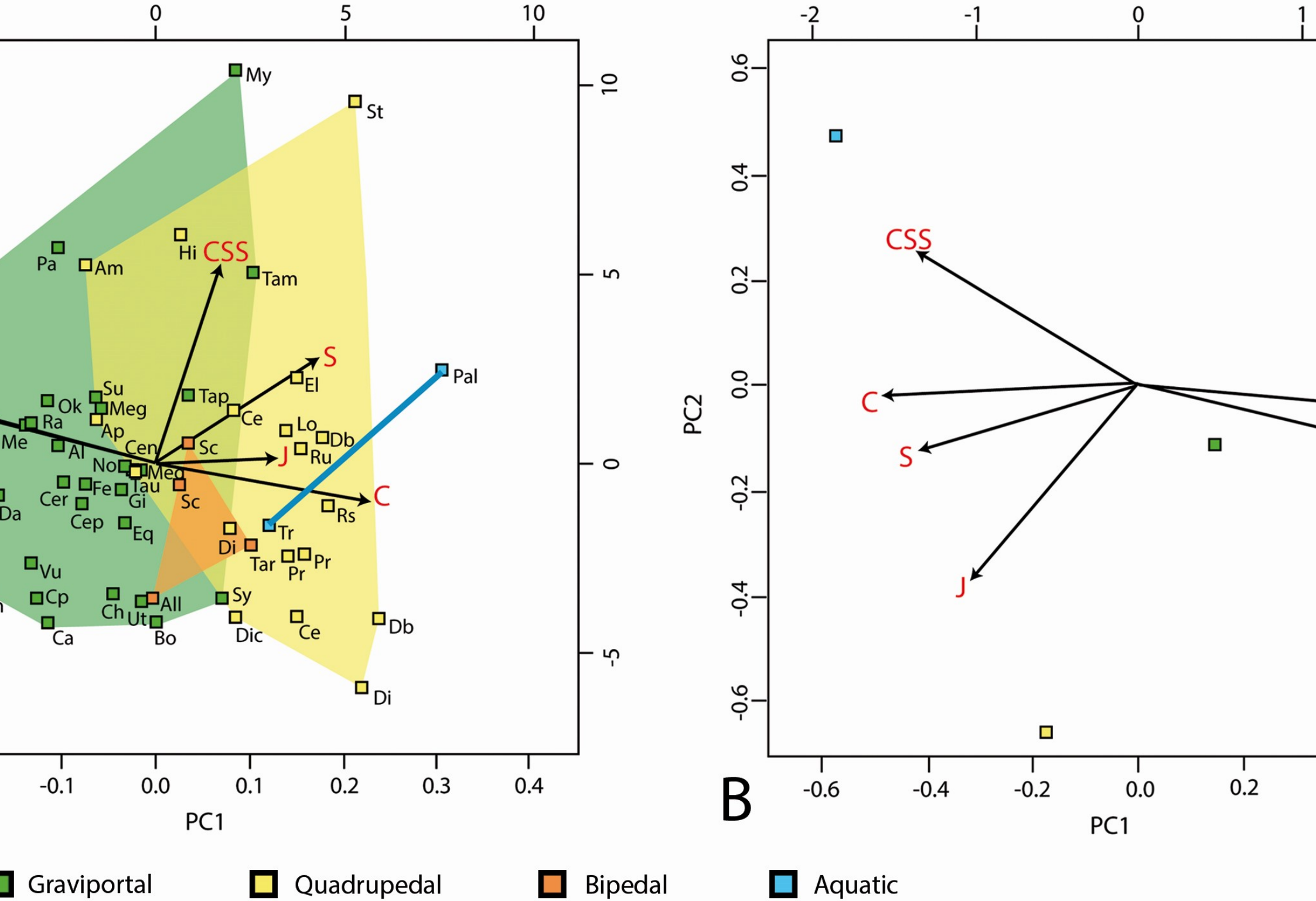
My
St
Hi
CSS
Pa
Am
Tam
S
Pal
El
Su
Tap
Ok
Meg
Ce
Ra
Lo
Db
Ap
Me
Al
Cen
Sc
J
Ru
No
Meg
Tau
Fe
C
Cer
Gi
Sc
Rs
Da
Cep
Eq
Tr
Di
Tar
Pr
Pr
Vu
Cp
Ch
All
Sy
Ut
Bo
Dic
Ce
Db
Ca
Di
0
5
10
10
5
0
-5
-0.1
0.0
0.1
0.2
0.3
0.4
PC1
-2
-1
0
1
0.6
0.4
0.2
0.0
-0.2
-0.4
-0.6
PC2
CSS
C
S
J
-0.6
-0.4
-0.2
0.0
0.2
PC1
B
Graviportal
Quadrupedal
Bipedal
Aquatic

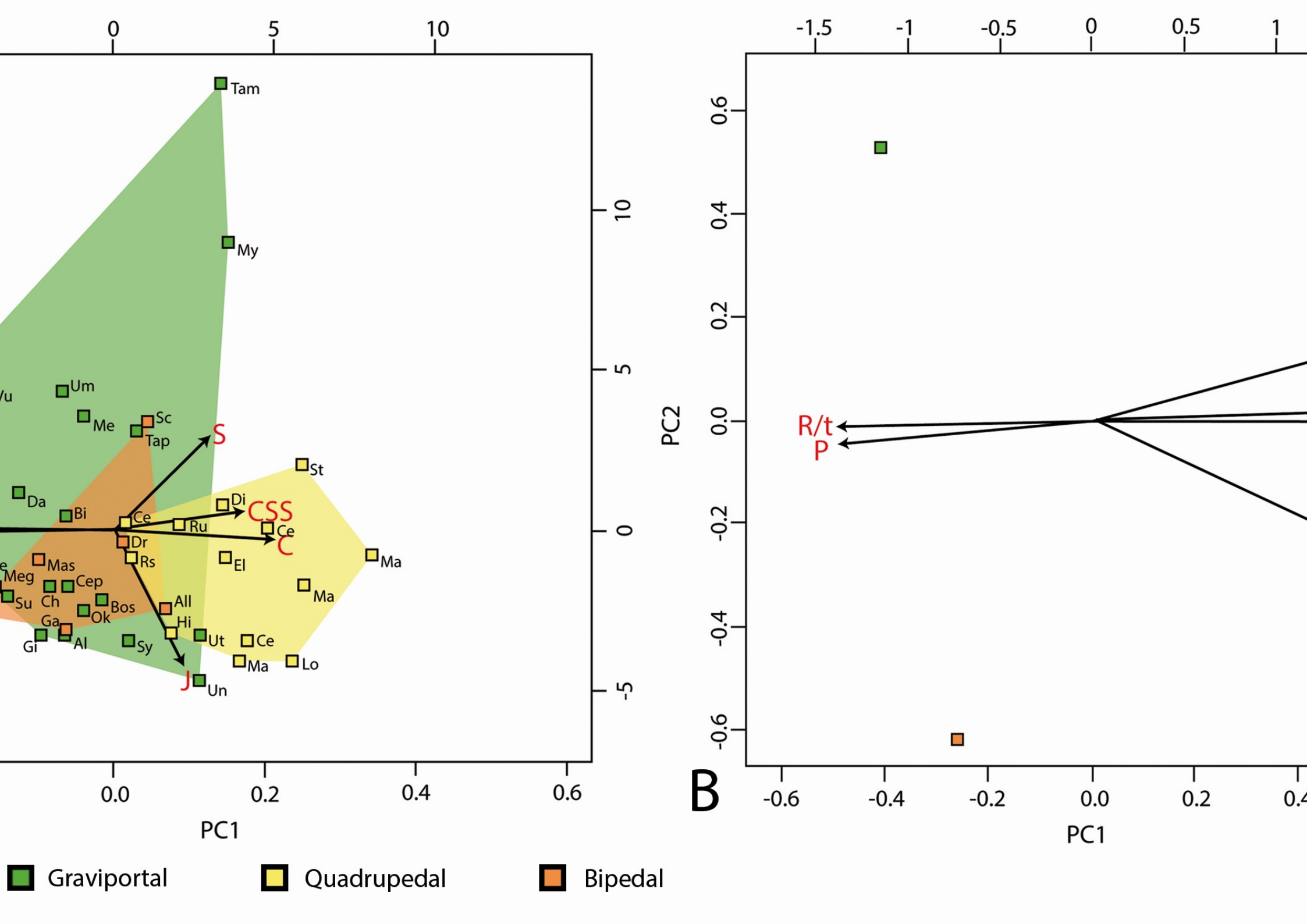
0
5
10
Tam
My
Um
Me
Sc
Tap
S
St
Da
Bi
Ce
Di
CSS
Ru
Ce
C
Dr
Rs
El
Ma
Mas
Meg
Cep
Ma
Su
Ch
Bos
All
Ok
Hi
Ga
Ut
Ce
Gl
Al
Sy
Ma
Lo
J
Un
10
5
0
-5
0.0
0.2
0.4
0.6
PC1
-1.5
-1
-0.5
0
0.5
1
0.6
0.4
0.2
0.0
-0.2
-0.4
-0.6
PC2
R/t
P
B
-0.6
-0.4
-0.2
0.0
0.2
PC1
Graviportal
Quadrupedal
Bipedal

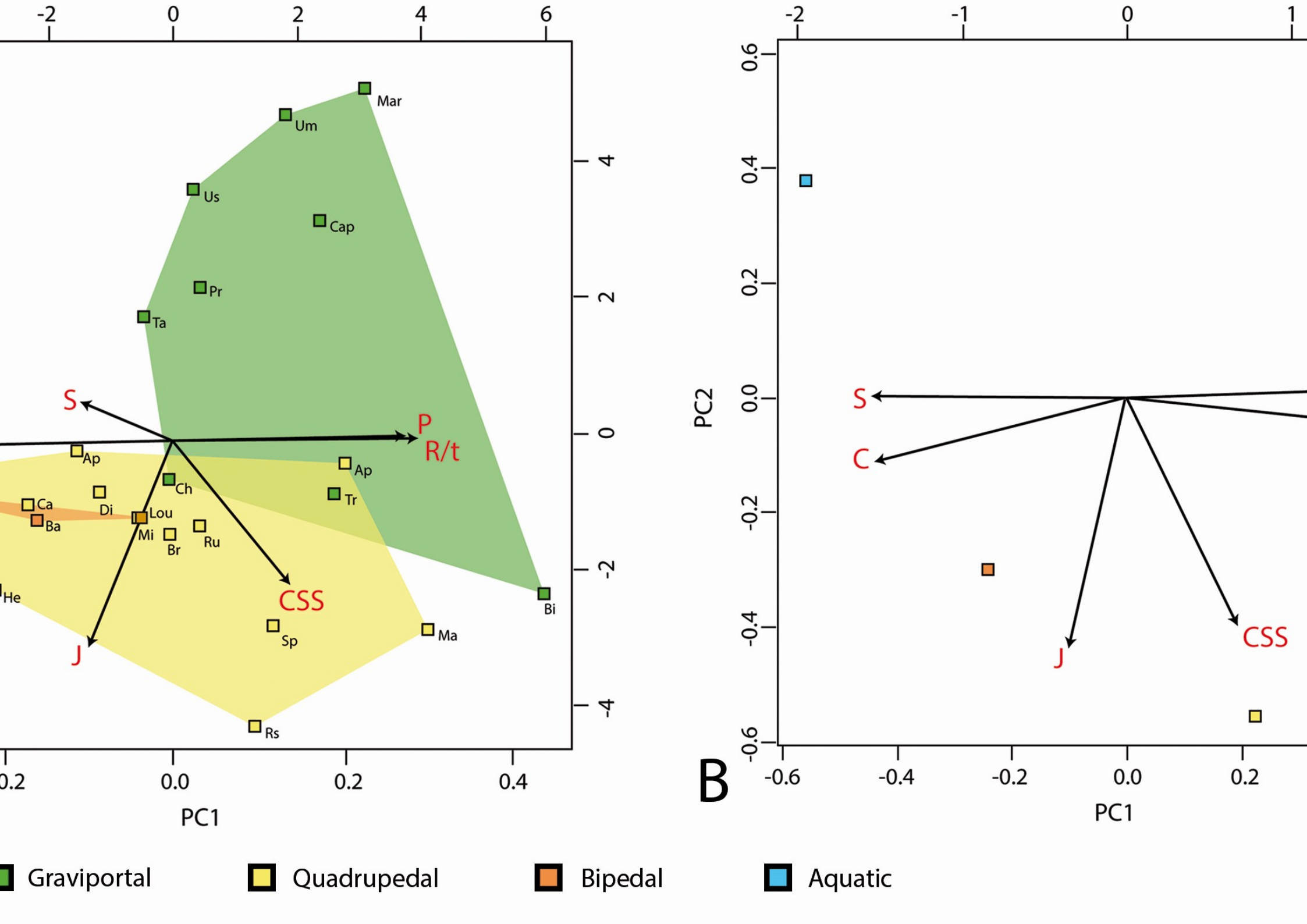
-2
0
2
4
6
Mar
Um
Us
Cap
Pr
Ta
S
P
R/t
Ap
Ch
Ap
Tr
Ca
Ba
Di
Lou
Mi
Br
Ru
He
CSS
Bi
Sp
Ma
J
Rs
4
2
0
-2
-4
0.2
0.0
0.2
0.4
PC1
B
-2
-1
0
1
0.6
0.4
0.2
0.0
-0.2
-0.4
-0.6
PC2
S
C
CSS
J
-0.6
-0.4
-0.2
0.0
0.2
PC1
Graviportal
Quadrupedal
Bipedal
Aquatic

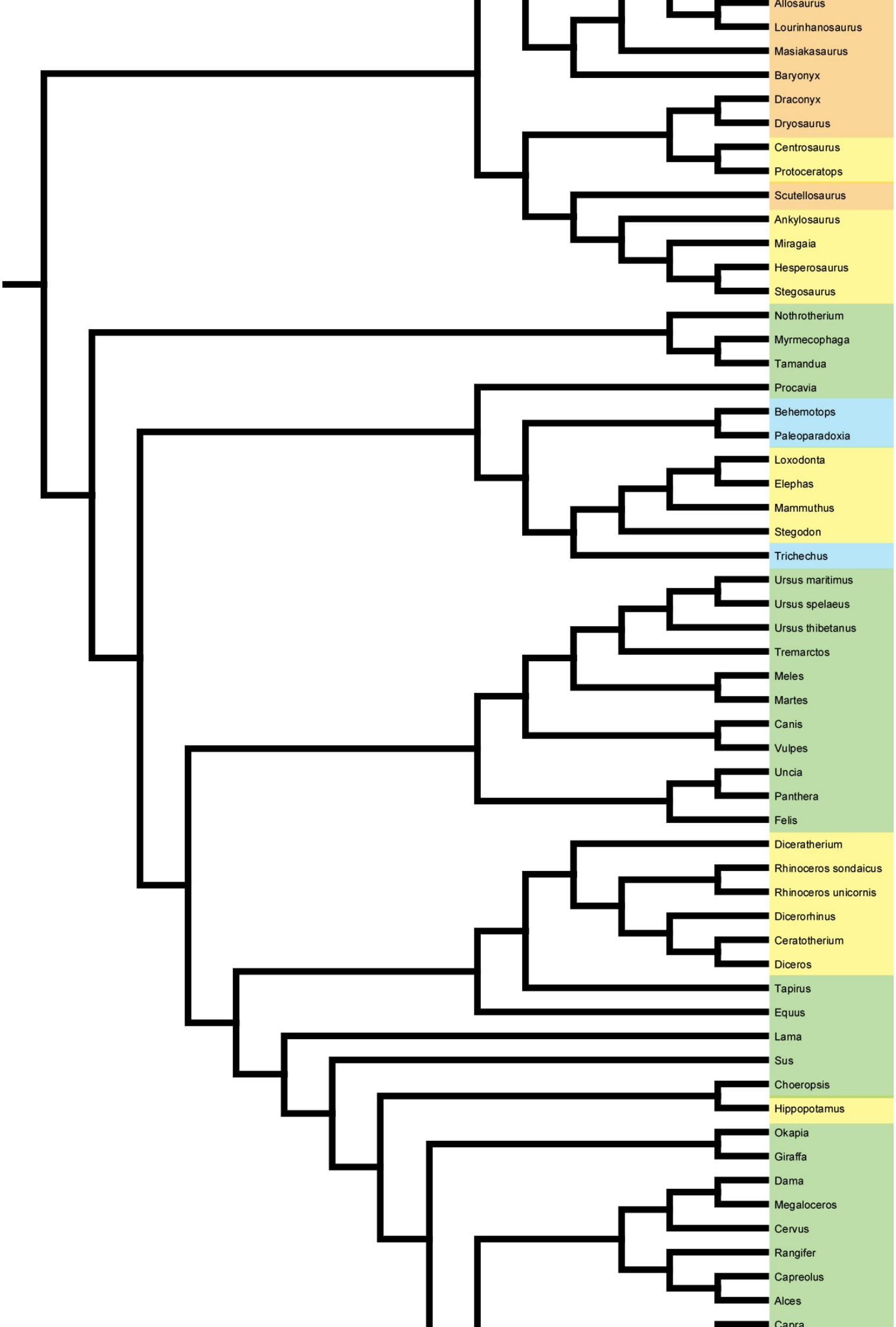
Allosaurus
Lourinhanosaurus
Masiakasaurus
Baryonyx
Draconyx
Dryosaurus
Centrosaurus
Protoceratops
Scutellosaurus
Ankylosaurus
Miragaia
Hesperosaurus
Stegosaurus
Nothrotherium
Myrmecophaga
Tamandua
Procavia
Behemotops
Paleoparadoxia
Loxodonta
Elephas
Mammuthus
Stegodon
Trichechus
Ursus maritimus
Ursus spelaeus
Ursus thibetanus
Tremarctos
Meles
Martes
Canis
Vulpes
Uncia
Panthera
Felis
Diceratherium
Rhinoceros sondaicus
Rhinoceros unicornis
Dicerorhinus
Ceratotherium
Diceros
Tapirus
Equus
Lama
Sus
Choeropsis
Hippopotamus
Okapia
Giraffa
Dama
Megaloceros
Cervus
Rangifer
Capreolus
Alces
Capra

	Phylogenetic Signal		Linear Regressions on the independent contrast data	
Humerus	K	p	p	adjusted R^2
C	0.68	<0.001*	0.91	-0.02
S	0.55	<0.001*	0.01*	0.11
P	0.49	<0.001*	0.81	-0.02
RT	0.56	<0.001*	0.50	-0.01
MD	0.40	<0.001*	-	-
CSS	0.34	0.041*	0.09	0.04
J	0.37	0.002*	0.04*	0.07
Femur				
C	0.46	<0.001*	0.01*	0.16
S	0.55	<0.001*	0.33	0.00
P	0.47	0.004*	0.01*	0.15
RT	0.48	0.003*	0.01*	0.13
MD	0.37	0.006*	-	-
CSS	0.51	0.007*	<0.01*	0.32
J	0.45	0.005*	<0.01*	0.54
Rib				
C	0.47	0.139	0.61	-0.03
S	0.39	0.550	0.15	0.05
P	0.65	0.016*	0.98	-0.04
RT	0.56	0.049*	0.47	-0.02
MD	0.67	0.017*	-	-
CSS	0.43	0.282	0.30	0.01
J	0.56	0.038*	<0.01*	0.35